Sign in

AMERICAN METEOROLOGICAL SOCIETY
AMS Journals Online

AMS Home | Journals Home | Journal Archive | Subscribe | For Authors | Help | Advanced Search | Search | Go

Full Text View

Volume 28, Issue 9 (September 1998)

Journal of Physical Oceanography
Article: pp. 1853–1860 | Abstract | PDF (117K)

Nonlinear Reflection of Internal Waves at a Density Discontinuityat the Base of the Mixed Layer

S. A. Thorpe

Department of Oceanography, Southampton Oceanography Centre, Southampton, United Kingdom

(Manuscript received April 25, 1997, in final form December 2, 1997)
DOI: 10.1175/1520-0485(1998)028<1853:NROIWA>2.0.CO;2

ABSTRACT

Internal waves propagating with an upward component of group velocity toward the ocean surface are reflected at the base of the mixed layer. A simple model is constructed to examine nonlinear aspects of the reflection. It consists of a uniform layer of depth h, representing the mixed layer, bounded above by a rigid surface and below by an interface, across which there is a density discontinuity $\Delta\rho$ and beneath which fluid is stably stratified with buoyancy frequency, N = const. Attention is given to the case in which an internal wave in the stratified layer, incident from below on the density interface, has frequency $\sigma < N/2$. In addition to a first-order wave of frequency σ that is reflected downward from the density discontinuity, a second-order wave is then generated with frequency 2σ and with horizontal wavenumber twice that of the incident wave, which also propagates downward away from the interface. The shape of the waves generated at the interface is investigated and a measure of their nonlinearity is defined. Highly nonlinear waves, with steeper slopes ahead of the wave crest than following it, are expected when the frequency of free interfacial waves with the same horizontal wavenumber as the incident wave is close or equal to σ and when the vertical wavelength of the incident waves is much greater than h.

The results are used to describe the nature of forced waves in the thermocline as supercritical internal waves propagate up a sloping boundary. The large soliton waves observed in the Bay of Biscay, where internal tidal waves propagating from their source at the shelf break encounter the thermocline, may be a consequence of the effects of nonlinear reflection.

Table of Contents:
- Introduction
- Theory
- Discussion
- REFERENCES
- APPENDIX
- FIGURES

Options:
- Create Reference
- Email this Article
- Add to MyArchive
- Search AMS Glossary

Search CrossRef for:
- Articles Citing This Article

Search Google Scholar for:
- S. A. Thorpe

1. Introduction

The problem to be addressed is that of the nonlinear reflection of a train of internal waves from a narrow thermocline separating a uniformly stratified region of constant buoyancy frequency N from a uniform upper ocean (or lake) mixed layer of depth h. This came to our attention when considering interactions that occur in the region where a stratified ocean or lake meets sloping boundaries and, in particular, when examining thermistor chain and CTD records made in summer in the stratified waters close to the shore of Lake Geneva over a sloping bottom boundary (e.g., see Thorpe and Jiang 1998). After a period of calm weather lasting for a week, oscillations persist in the almost uniform stratification of the deeper water with

amplitudes of 1–2 m. The strongly stratified seasonal thermocline is relatively unperturbed. It is known from the theoretical work of Phillips (1966) and Eriksen (1985) and from laboratory experiments of waves incident on slopes (Cacchione and Wunsch 1974; Thorpe 1987; Taylor 1993) that internal waves impinging on a sloping boundary may, on reflection, be amplified and propagate upward through the stratified thermocline toward the mixed layer. Waves having the form of a wave mode in deeper water are decomposed on reflection so that, after reflection, those traveling toward the mixed layer are more appropriately described as rays. A condition for internal wave propagation is that the wave frequency σ is less than N; the inclination of an internal wave ray path to the horizontal (or the angle between the group velocity vector and the horizontal) is $\sin^{-1}(\sigma/N)$ (Phillips 1966). But what happens to the ray when it reaches the high density gradient boundary of the stratified region and cannot propagate upward farther into the overlying mixed layer where N is less than the wave frequency? It may reflect if N gradually decreases below σ as depth decreases, as demonstrated by theory and laboratory experiments by Nicolaou et al. (1993). Moreover, a linear theory and experiments of Delisi and Orlanski (1975), described below, show reflection occurs at a density interface bounding a stratified region in which internal waves propagate. But how do nonlinear terms affect reflection? Can waves over a shallowing bottom, perhaps after successive reflections at a density interface and at the sloping lower boundary (where their wavenumbers and amplitudes are changed), reach a critical condition in which their interaction with the high density gradient in the thermocline becomes very large?

Our interest in the subject comes also from the intriguing observations of Holligan et al. (1985) and New and Pingree (1990, 1992). Some 140–150 km away from the shelf break in the deep water of the Bay of Biscay they find large amplitude internal waves, usually two or three, with deep troughs and relatively broad crests resembling those found in soliton packets. The waves travel in directions away from the shelf break. It is curious that, in general contrast to observations elsewhere of internal wave soliton packets, there are so few waves observed and that the waves are confined to a local region. New and Pingree argue convincingly that these thermocline waves owe their presence to internal tidal waves. Generated at the shelf break by the interaction of the barotropic tide with the topography, these internal waves propagate downward as a ray, which is well documented by observations and a numerical model by New (1988). The ray meets and reflects from the sea bed at depths of some 3.8 km (where the interaction with the benthic boundary layer may raise questions related to those considered here; see also d'Asaro 1982). The waves then propagate upward toward the seasonal thermocline. They are predicted to encounter the upper layers of the ocean in the vicinity of the location at which the large internal waves are observed in the center of the Bay of Biscay. New and Pingree remark that numerical experiments with New's linear model show that the amplitudes of these waves are approximately double those found near of the shelf break. In view of the recent increased interest in the properties and long range propagation of internal tides (Dushaw et al. 1995; Morozov 1995; Munk 1998), it is of importance to understand those processes that may affect their propagation and detection, one of which is the interaction with the thermocline.

The elegant laboratory experiments and linear theory of Delisi and Orlanski (1975) provide very useful insights into the dynamics of wave reflection from an interface between two layers of stratified and nonstratified water across which there is a density discontinuity $\Delta\rho$. If dissipation is negligible, the energy flux of the waves must be conserved. A reflected internal wave ray is therefore generated of amplitude equal to the incident wave and, since it has the same frequency as the incident wave, the reflected wave travels downward from the interface at the same angle below the horizontal as the incident wave has above it. The reflected wave does not, in general, have the same phase as the incident wave. The interface between the layers is perturbed as a consequence of reflection, and an interfacial wave is locally forced in the region of the reflecting ray. Photographs of the experiments show the interfacial wave to be largely confined to the region where the ray is incident on the interface. The phase of the interfacial wave advances in the same direction as the horizontal phase velocity component of the incident internal wave. The interfacial wave has an amplitude (in the linear theory) that depends on a ratio σ/σ_0. Here σ is the frequency of the incident wave frequency and σ_0 is a frequency that depends on the density difference across the interface. (Delisi and Orlanski use the ratio of the horizontal phase speeds instead of σ/σ_0, but the two ratios are equal since the phase speed is σ/k. However σ_0 is not, as suggested by Delisi and Orlanski, the frequency of interfacial waves that may travel along the interface with the same horizontal wavenumber as the incident waves—see section 2a.) When $\sigma = \sigma_0$, the interfacial waves have their maximum amplitude, twice that of the incident wave, and the incident and reflected waves in the stratified layer have the same phase.

Delisi and Orlanski do not provide any evaluation of nonlinear effects on, for example, the amplitude of the interfacial waves. When N is constant below the interface, as supposed here for simplicity, both the incident and the reflected waves may be described by linear solutions of the equation of motion, which are exact; no terms in the equations of motion are discarded other than those of dissipation, which we shall neglect here, and the solutions are valid even when the waves are of such large amplitude that they develop regions of static instability. Such solutions are not, however, available for the interfacial waves, and an objective is therefore to investigate, using a conventional approximation scheme, the nonlinear terms that affect the form of the interfacial waves during reflection.

2. Theory

a. First-order solution

The model is that shown in Fig. 1. The upper "mixed layer" is homogeneous of uniform density ρ_1 and of mean depth h, topped by a rigid boundary at $z = h$. There is a density increase, $\Delta\rho$, across the interface at $z = 0$, below which the density increases steadily downward and the buoyancy frequency N is constant. For simplicity, the effects of rotation are ignored. The phase and group velocities of internal gravity waves have opposite directions of propagation in the vertical. A plane internal wave with phase vector $(k, -m)$ with k and $m > 0$, traveling with a positive upward component of group velocity in

the x–z plane, is incident on the interface and is represented by a streamfunction $\psi_I = a\cos(kx - mz - \sigma t)$. This form of the streamfunction is an exact progressive wave solution of the inviscid equations of motion when the Boussinesq approximation is valid (Thorpe 1994a). The perturbed density is equal to

$$\rho_0\{1 - (N^2/g)[z - (ak/\sigma)\cos(kx - mz - \sigma t)]\},$$

or $\rho_0[1 - (N^2z/g)] + \rho_I$, where ρ_0 is a mean reference density and ρ_I is the density perturbation at (x, z) and time t, caused by the incident wave. The angle that the group velocity makes with the horizontal is $\beta = \sin^{-1}(\sigma/N)$, and the dispersion relation is $\sigma^2 = N^2k^2/(k^2 + m^2)$. Although the density perturbation is sinusoidal, the isopycnal surfaces are not, except at very small amplitude. The waves on the isopycnal surfaces have steeper forward faces than rear faces, where "forward" means ahead of the wave crest, which advances in the x direction and is therefore the horizontal direction of phase advance. The appropriate measure of wave steepness is Am (Thorpe 1994a), where $A = ak/\sigma$ is the amplitude of the vertical fluctuations in the density field caused by the waves. If $Am = 1$, isopycnal surfaces become vertical somewhere in the wave field. They overturn if $Am > 1$.

Following Delisi and Orlanski (1975) we can find a solution that represents motion and density perturbations in the three parts of the system and satisfies the condition of zero vertical velocity at $z = h$ and also the *linearized* kinematic and pressure boundary conditions at the interface, that particles follow the interface and that pressure is continuous, respectively. The solution consists of a reflected wave with streamfunction ψ_{R1} and density perturbation ρ_{R1} below the interface, an interfacial wave $z = \eta_1(x, t)$, and a forced motion with velocity potential ϕ_1 in the homogeneous layer above the interface. The velocity potential satisfies Laplace's equation and the boundary condition $w = \partial\phi_1/\partial z = 0$ at $z = h$. The solution for the reflected streamfunction is

$$\psi_{R1} = a\cos(kx + mz - \sigma t + \gamma), \qquad (1)$$

where $\tan(\gamma) = 2t_\beta t_{kh}p/(t^2_{kh} - p^2t^2_\beta)$ with $t_\beta = \tan(\beta)$, $t_{kh} = \tanh(kh)$, and $p = [1 - \sigma^2_0/\sigma^2]$ where $\sigma^2_0 = gk\Delta\rho t_{kh}/\rho_0$. The latter is not the dispersion relation of interfacial waves traveling along the interface between uniform density layers, which is $\sigma^2 = gk\Delta\rho t_{kh}/(\rho_0 t_{kh} + \rho_1)$, where ρ_1, ρ_2 are the densities of the upper and lower layers, respectively; see LeBlond and Mysak (1978). Nor is it the dispersion relation of interfacial waves on an interface between a uniform and a stratified layer, as is the physical situation here. (The dispersion relation for $\sigma > N$ is then found to be

$$\sigma^2 = gk\Delta\rho t_{kh}/[\rho_1 + \rho_0 t_{kh}(1 - N^2/\sigma^2)^{1/2}].$$

There is no unique dispersion relation if $\sigma < N$.) The amplitudes of the incident and reflected waves (i.e., the amplitudes of the vertical displacements of isopycnal surfaces) are both equal to $A = ak/\sigma$. When $p = 0$ (i.e., when $\sigma = \sigma_0$), the angle $\gamma = 0$, and the incident and reflected waves are in phase. The reflected streamfunction (1) is, like the incident wave, an exact solution of the equations of motion but the slope of forward faces of its isopycnal surface displacements (ahead of the wave crests) is less than the rear. The displacement of the interface at the foot of the mixed layer is sinusoidal at this first order and is given by

$$\begin{aligned}\eta_1 &= 2A[t_{kh}/(t^2_{kh} + p^2t^2_\beta)] \\ &\quad \times \{t_{kh}\cos(kx - \sigma t) - pt_\beta\sin(kx - \sigma t)\} \\ &= 2A\cos\alpha_1\cos(kx - \sigma t + \alpha_1), \qquad (2)\end{aligned}$$

where $\alpha_1 = \tan^{-1}(pt_\beta/t_{kh})$ (taking the principal value) is the phase of the interfacial wave relative to that of the incident wave. When $p = 0$, the amplitude of the interfacial wave is equal to $2A$, twice that of the incident wave, and the phase difference, α_1, is zero. Equation (2) is a first-order, and not an exact, solution for the interface displacement.

In the experiments conducted by Delisi and Orlanski, internal waves generated by a horizontal paddle arrangement propagate in rays through a uniformly stratified layer to reflect from an interface beyond which the density is uniform. This reproduces completely the geometry of the analytical model, except that it proved more convenient for the incident waves to propagate downward through a uniform stratification beneath which was an interface and mixed layer; the laboratory model is the inverse of that shown in Fig. 1 but the dynamics are the same. Experiments are run with $h = 0.45(\pm 0.005)$ m and $2\pi/k = 0.24$ m, so that t_{kh} is always close to unity. The buoyancy frequency ranges from 0.72 to 0.84 s^{-1}, and the wave frequencies from 0.42 to 0.72 s^{-1}, and β ranges from 33° to 62°. The parameter p is varied from about −60 to unity, mainly by varying the density differences across the interface. The interfacial wave slopes, $k|\eta_1|$, are less than 0.5. Interfacial phase and amplitude are examined as functions of $\Delta\rho/\rho_0$. The agreement between the linear theory and observations is fairly good, demonstrating the trends predicted by the theory, with phase agreeing to within about 30° and amplitude to typically about ±50%. Delisi and Orlanski observe the development of regions of static instability within the region of overlap of the incident

and reflected rays that, from their orientation, appear to be a manifestation of the small-scale parametric instability often observed in laboratory experiments on internal waves and explained by McEwan and Robinson (1975) to be associated with subharmonic frequencies, $\sigma/2$ (see also Mied 1975; Thorpe 1994b). They do not appear to affect the density interface, our focus of attention, and are not considered further here.

b. Second-order solution

Second-order effects are accounted for in the now conventional way of seeking a solution of the equations of motion and the boundary conditions as a perturbation about the first-order solution (see e.g., Thorpe 1968, 1987). If ψ_{R2}, Φ_2, and η_2 are the second-order streamfunction below the interface, the second-order velocity potential in the mixed layer and the second-order interface perturbation, respectively, then it may be shown that ψ_{R2} must satisfy the linear equation

$$[\partial^2\nabla^2/\partial t^2 + N^2\partial^2/\partial x^2]\psi_{R2} = 0, \quad (3)$$

where ∇^2 is the Laplace operator, $\partial^2/\partial x^2 + \partial^2/\partial z^2$. All first-order product order terms vanish indentically and ψ_{R1} satisfies (3). The velocity potential Φ_2 must, like Φ_1, satisfy Laplace's equation and the boundary condition $\partial\Phi_2/\partial z = 0$ at $z = h$. All the nonlinearity derives from the boundary conditions at the interface. The boundary conditions are given in appendix A. The solution is straightforward. The second-order terms are forced by products of first-order terms, leading to second-order terms with phase proportional to $2(kx - \sigma t)$. Equation (3) then implies that ψ_{R2} is proportional to $\exp[2i(kx + m_2 z - \sigma t)]$, where $m^2_2 = k^2(N^2 - 4\sigma^2)/4\sigma^2$. This wavenumber can also be written as $m_2 = (m/2)(1 - 3t^2_\beta)^{1/2}$. If $\sigma > N/2$ (or equivalently $\beta > \pi/6$), m_2 is imaginary and the forced second-order reflected component is an evanescent mode, decaying exponentially with distance below the interface. (Similar evanescent reflected modes are found in internal waves reflecting from a slope; Thorpe 1987). If, however, $\sigma < N/2$ (i.e., if $\beta < \pi/6$ or 30°), this forced reflected component is a free wave propagating downward from the interface when the positive root for m_2 is taken. We shall here suppose that $\sigma < N/2$, which is the case most applicable to the ocean and lakes, although not that which corresponds to the experiments by Delisi and Orlanski where larger values of β are used.

Expressions for the amplitude $|\eta_2|$ and the phase α_2 of the second-order interfacial wave displacements, so that $\eta_2 = |\eta_2| \cos[2(kx - \sigma t) + \alpha_2]$, are given in appendix B. The natural expansion for interfacial waves is in terms of the first-order wave slope (Hunt 1961; Thorpe 1968). A measure of the nonlinearity of the interfacial waves, χ, is given by the ratio of the second-order amplitude to that of the first, divided by the wave slope of the first order wave, $k|\eta_1|$; $\chi = |\eta_2|/k|\eta_1|^2$. This may be written in terms of m since $k = mt_\beta$.

3. Discussion

a. Nonlinearity and wave shape

Values of χ and the difference in the phase angles, $\gamma = (\alpha_1 - \alpha_2/2)$, of the first- and second-order interfacial displacements are plotted in Figs. 2 and 3, respectively, for various values of p, t_β, and t_{kh}. The angle γ is a measure of the distortion of the first-order sinusoidal wave shape by the superposition of the second-order terms. If $\gamma = 0$, the troughs are flattened and the peaks narrower. When $\gamma = \pi/2$, the waves have narrow troughs and flattened peaks. If $0 < \gamma < \pi/2$, the forward face of the waves is steeper than the rear face, while the contrary holds true when $\pi/2 < \gamma < \pi$. The behavior is cyclic with period π so that, for example if $\gamma = -\pi/2$, the waves again have narrow troughs and flattened peaks. At $p = 0$ [i.e., $\sigma = \sigma_0$, and when the first-order interface displacement has its largest value, $\eta_1 = 2A\cos(kx - \sigma t)$], the second-order interfacial wave displacement is

$$\eta_2 = A^2k\{(3t^2_{kh} - t^2_\beta t^2_{kh} - 2t^2_\beta)/[t_\beta t^2_{kh}(1 - 3t^2_\beta + t^2_\beta t^2_{kh})]\}[t_{kh}t_\beta \cos 2(kx - \sigma t) - (1 - 3t^2_\beta)^{1/2}\sin 2(kx - \sigma t)], \quad (4)$$

(Click the equation graphic to enlarge/reduce size)

or, if both t_β (= k/m) and $t_{kh} \ll 1$, (when $t_{kh} \approx kh$)

$$\eta_2/2A = Am[3/2 - (mh)^{-2}]\sin 2(kx - \sigma t). \quad (5)$$

Here $|\eta_2|/2A$ is approximately equal to $3Am/2$ if $mh \gg 1$; that is, if the inverse wavenumber of the incident internal wave, m^{-1}, is much smaller than the thickness of the upper mixed layer, h. The interfacial wave then has steeper slopes ahead of the wave crest than following it and so resembles the shape of the incident internal wave, but the perturbation from sinusoidal is generally small if the incident wave steepness, Am, is small. If, however, $mh \ll 1$ (i.e., when the vertical wavelength of the incident internal wave, $2\pi m^{-1}$, is much greater than the thickness of the upper mixed layer), $|\eta_2|/2A$ is approximately equal to $Am/(mh)^2$, which may be of order unity, even when the slope of the incident wave, Am, is small. The

wave shape is asymmetrical with steeper slopes following the wave crest than in front of it. In this case $\chi = 1/(2kmh^2)$. Figure 2a shows the variation of χ with p at $t_\beta = 0.1$ and at $t_{kh} = 0.03$, 0.1, and 0.3. When $p = 0$ and $t_{kh} = 0.03$, then $mh = 0.3$ and χ has large values as predicted. Figure 2b shows how γ, and therefore the wave shape, varies for the same set of parameter values.

If $p \ll -1$ (i.e., when $|p| \gg 1$ or $\sigma \ll \sigma_0$), $\eta_1 \approx -[2At_{kh}/pt_\beta] \sin(kx - \sigma t)$, $\eta_2 \approx -[p/4t_{kh}k\,|\eta_1|^2] \cos 2(kx - \sigma t)$ and $\chi \approx |p|/2t_{kh}$. This tends to infinity, as indicated by the increasing values of χ at large negative p in Fig. 2a. The waves have flattened crests and narrow troughs but, since $|\eta_1|$ is small compared to the incident wave amplitude at large negative p, the amplitude of the interfacial waves is small even though the nonlinearity is great; the mismatch of natural frequences of the incident and interfacial wave makes the interface relatively unresponsive to the forcing by the incident wave. For comparison, Fig.3 shows the variation in χ and γ at $p = 0.2$ as t_{kh} varies from 0 to 1 for $t_\beta = 0.1$, 0.2, and 0.4. Large values of χ occur at sufficiently small t_β, as expected.

b. Waves traveling over a slope toward a thermocline

Supercritical internal waves approaching a slope from deep water, and reflecting and continuing with a positive component toward shallow water, will be reflected downward from an overlying thermocline. The second-order component with frequency 2σ will be either evanescent and therefore trapped in the vicinity of the thermocline if $\beta > \pi/6$ or free if $\beta < \pi/6$. If the latter, it (and higher-order components) will travel at a *steeper* angle to the horizontal than the incident or first-order reflected wave but with the same group speed. It will therefore lag *behind* the linear component in its propagation toward shallow water; the thermocline reflection does not lead to a mechanism that reduces the time of travel of the internal waves toward shore. On each reflection from the bottom the horizontal wavenumber component will increase. The frequency σ_0 will therefore increase, and $p = [1 - \sigma^2_0/\sigma^2]$ will decrease since σ remains constant, p eventually becoming large and negative. The amplitude of the first-order wave on the thermocline is then proportional to $2A/pt_\beta$ [see (2)] and, since p is proportional to $-k$, its change as the internal wave proceeds toward shore will depend on A/k, provided the density distribution, so t_β and thermocline depth remain the same. However, on internal wave reflection from a sloping boundary, A/k is conserved (Eriksen 1985) so that little change in the amplitude of the forced thermocline displacement may occur as waves approach shore, at least after the position is passed where $p = 0$, although because the wavenumber k increases, they will become progressively steeper. The nonlinear terms examined here do not appear to lead to significant processes occurring at the interface except perhaps for waves with $p > 0$ in deep water for which p may become close to zero after reflection at the bottom. For waves with $p < 0$ in deep water, wave breaking is most likely to occur as a consequence of wave steepening on reflection at the sloping bottom.

c. Waves in the Bay of Biscay

New's (1988) linear numerical model of the internal tides in the Bay of Biscay shows the internal wave ray propagating at an angle of about 1 in 25 to the horizontal, so $t_\beta = 0.04$. The internal waves observed in the center of the bay by New and Pingree are 1–2 km in wavelength, and the mixed layer is about 50 m deep. These values give values of t_{kh} of about 0.156 to 0.304, and so $p, = 1 - gk\Delta\rho t_{kh}/\sigma^2\,\rho_0$, is approximately $1 - (2.5 - 9.7) \times 10^5\,\Delta\rho/\rho_0$. This is large and negative for typical fractional density differences corresponding to the 2–4°C temperature across the seasonal thermocline. While χ may therefore be large (Fig. 2a), the first-order interface displacement will be small compared to the incident wave amplitude. When, however, the horizontal scale of the internal tidal waves is as small as 1–2 km, their vertical scale will be only 40–80 m; this makes untenable the assumption that the thermocline can be represented by a step change in density. If alternatively the incident internal tidal waves have horizontal scales of 10–15 km, their vertical scale will greatly exceed the thermocline thickness, $gk\Delta\rho t_{kh}/\sigma^2\rho_0$ is of order unity, and consequently p is near zero, γ is near $3\pi/4$, and χ is large (Fig. 2). The interfacial wave amplitude is about twice that of the incident wave, second-order terms are large, and the backward facing slope of the waves will be steeper than the forward slope. The development of soliton packets as found on the continental slope (e.g., Small et al. 1998) is to be expected. More information is required about the vertical and horizontal scale of the internal tidal ray in the center of the bay before the processes operating in the reflection region of the thermocline can be properly assessed.

In this simplistic analysis we have, however, ignored several factors. These include the higher-order terms that may affect wave shape, small disturbances and instabilities (e.g., those related to parametric instability that may affect the reflection process), and the narrow beam structure of the incident wave. Two other effects that may affect the amplitude or shape of the internal waves, the earth's rotation with its consequent Coriolis effects and dissipation, have not been taken into account. All these should be carefully assessed in a more thorough comparison with particular observations.

Acknowledgments

I am grateful to Mr. A. Nimmo-Smith for producing Figs. 2 and 3 and to a referee for suggesting corrections to the text and for noticing a term previously omitted in Eq. (A5).

REFERENCES

Cacchione, D., and C. Wunsch, 1974: Experimental study of internal waves over a slope. *J. Fluid Mech.,* **66,** 223–240..

D'Asaro, E. A., 1982: Absorption of internal waves by the benthic boundary layer. *J. Phys. Oceanogr.,* **12,** 323–336..

Delisi, D. P., and I. Orlanski, 1975: On the role of density jumps in the reflection and breaking of internal gravity waves. *J. Fluid Mech.,* **69,** 445–464..

Dushaw, B. D., B. D. Cornuelle, P. F. Worcester, B. M. Howe, and D. S. Luther, 1995: Barotropic and baroclinic tides in the Central North Pacific determined from long-range reciprocal acoustic transmissions. *J. Phys. Oceanogr.,* **25,** 631–647..

Eriksen, C. C., 1985: Implications of ocean bottom reflection for internal wave spectra and mixing. *J. Phys Oceanogr.,* **15,** 1145–1156..

Holligan, P. M., R. D. Pingree, and G. T. Mardell, 1985: Oceanic solitons, nutrient pulses and phytoplankton growth. *Nature,* **314,** 348–350..

Hunt, J. N., 1961: Interfacial waves of finite amplitude. *La Houille Blanche,* **4,** 515–531..

LeBlond, P. H., and L. A. Mysak, 1978: *Waves in the Ocean.* Elsevier, 602 pp..

McEwan, A. D., and R. M. Robinson, 1975: Parametric instability of internal gravity waves. *J. Fluid Mech.,* **67,** 667–687..

Mied, R. P., 1976: The occurrence of parametric instability in finite-amplitude internal gravity waves. *J. Fluid Mech.,* **78,** 763–784..

Morozov, E. G., 1995: Semidiurnal internal wave global field. *Deep-Sea Res.,* **42,** 135–148..

Munk, W., 1998: *Twice Again—Tidal Friction.* in press..

New, A. L., 1988: Internal tidal mixing in the Bay of Biscay. *Deep-Sea Res.,* **35,** 691–709..

— ~~, a~~nd R. D. Pingree, 1990: Large amplitude internal soliton wave packets in the Bay of Biscay. *Deep-Sea Res.,* **37,** 513–524..

— ~~,—~~ ~~, 1~~992: Local generation of internal soliton packets in the central Bay of Biscay. *Deep-Sea Res.,* **39,** 1521–1534..

Nicolaou, D., R. Liu, and T. N. Stevenson, 1993: The evolution of thermocline waves from an oscillatory disturbance. *J. Fluid Mech.,* **254,** 401–416..

Phillips, O. M., 1966: *Dynamics of the Upper Ocean.* Cambridge University Press. 261 pp..

Taylor, J. R., 1993: Turbulence and mixing in the boundary layer generated by shoaling internal waves. *Dyn. Oceans Atmos.,* **19,** 233–258..

Thorpe, S. A, 1968: On the shape of progressive internal waves. *Philos. Trans. Roy. Soc. London A,* **263,** 564–614..

— ~~, 1~~987: On the reflection of a train of finite amplitude internal waves from a uniform slope. *J. Fluid Mech.,* **178,** 278–302..

— ~~, 1~~994a: Statically unstable layers produced by overturning internal gravity waves. *J. Fluid Mech.,* **260,** 333–350..

— ~~, 1~~994b: Observations of parametric instability and breaking waves in an oscillating tilted tube. *J. Fluid Mech.,* **261,** 33–45..

— ~~, a~~nd R. Jiang, 1998: Estimating internal waves and diapycnal mixing from conventional mooring data in a lake. *Limnol. Oceanogr.,* in press..

APPENDIX A

4. Second-Order Boundary Conditions

To second order, the kinematic boundary conditions for the lower and upper layer are

$$\partial(\eta_1 + \eta_2)/\partial t + (u_I + u_{R1})\partial\eta_1/\partial x = w_I + w_{R1} + w_{R2} \quad \text{(A1)}$$

and

$$\partial(\eta_1 + \eta_2)/\partial t + (u_1 + u_2)\partial\eta_1/\partial x = w_1 + w_2, \quad \text{(A2)}$$

respectively, both evaluated at $z + \eta_1 + \eta_2$. Here w is the vertical velocity component, and the u and w subscripts follow the convention already adopted. Expanding about $z = 0$ and recalling the equality of first-order terms gives

$$\partial\eta_2/\partial t + \partial\psi_{R2}/\partial x = -\partial\eta_1/\partial x[\partial\psi_I/\partial z + \partial\psi_{R1}/\partial z] - \eta_1[\partial^2\psi_I/\partial x\partial z + \partial^2\psi_{R1}/\partial x\partial z] \quad \text{(A3)}$$

and

$$\partial\eta_2/\partial t - \partial\phi_2/\partial z = -\partial\eta_1/\partial x(\partial\phi_1/\partial x) + \eta_1\partial^2\phi_1/\partial z^2, \quad \text{(A4)}$$

respectively, each evaluated at $z = 0$.

The pressure boundary condition is found by equating the pressure gradients in the upper and lower fluids along the interface. The pressure gradient is

$$\partial p/\partial x = \partial\eta/\partial x(\partial p/\partial z)$$

at $z = \eta$. Using the equations of motion in the lower layer and the (exact) Bernoulli equation for the pressure in the upper layer, expanding about $z = 0$, and discarding terms that balance at first order we find, at second order,

$$\begin{aligned}
&\partial^2\psi_{R2}/\partial t\partial z + g(\Delta\rho/\rho_0)\partial\eta_2/\partial x - \partial^2\phi_2/\partial t\partial x \\
&= \eta_1\partial^3\phi_1/\partial t\partial x\partial z + (\partial/\partial x)[(\partial\phi_1/\partial x)^2 + (\partial\phi_1/\partial z)^2]/2 - \eta_1(\partial^3/\partial t\partial z^2)(\psi_I + \psi_{R1}) - (\partial/\partial z)(\psi_I + \psi_{R1})[(\partial^2/\partial x\partial z)(\psi_I + \psi_{R1})] \\
&\quad + (\partial/\partial x)(\psi_I + \psi_{R1})[(\partial^2/\partial z^2)(\psi_I + \psi_{R1})] - g[(\rho_I + \rho_{R1})/\rho_0]\partial\eta_1/\partial x + (\partial\eta_1/\partial x)[(\partial^2/\partial x\partial t)(\psi_I + \psi_{R1}) + \partial^2\phi_1/\partial z\partial t],
\end{aligned} \quad \text{(A5)}$$

(Click the equation graphic to enlarge/reduce size)

evaluated at $z = 0$. The terms on the rhs of (A3)–(A5) are derived from the solutions found at first order.

APPENDIX B

5. The Second-Order Solution for the Interfacial Waves, η_2

When $\beta < \pi/6$,

$$\eta_2 = A_1[B_1 \cos(2(kx - \sigma t) - B_2 \sin 2(kx - \sigma t)], \quad \text{(B1)}$$

where

$$A_1 = k|\eta_1|^2/\{4t_{kh}t_\beta[t_{kh}^2(1 - 3t_\beta^2) + t_\beta^2(p + t_{kh}^2)^2](t_{kh}^2 + p^2t_\beta^2)\}, \quad \text{(B2)}$$

$$\begin{aligned}
B_1 = t_\beta\langle(p^2t_\beta^2 - t_{kh}^2)[2pt_{kh}^2(1 - 3t_\beta^2) + (p + t_{kh}^2)\{t_\beta^2(2 + t_{kh}^2 - p^2) - 3t_{kh}^2\}] \\
- 2pt_{kh}^2(1 - 3t_\beta^2)^{1/2}[t_\beta^2(2 + t_{kh}^2 - p - 2p^2 - 2pt_{kh}^2) - 3t_{kh}^2]\rangle,
\end{aligned} \quad \text{(B3)}$$

and

$$\begin{aligned}
B_2 = -t_{kh}\langle(p^2t_\beta^2 - t_{kh}^2)(1 - 3t_\beta^2)^{1/2}[2t_\beta^2 + t_{kh}^2t_\beta^2(1 - 2p) - 3p^2t_\beta^2 - 3t_{kh}^2] \\
+ 2pt_\beta^2[2pt_{kh}^2(1 - 3t_\beta^2) + (p + t_{kh}^2)\{(2 + t_{kh}^2)t_\beta^2 - 3t_{kh}^2 - p^2t_\beta^2\}]\rangle.
\end{aligned} \quad \text{(B4)}$$

(Click the equation graphic to enlarge/reduce size)

Hence,

$$\eta_2 = |\eta_2| \cos[2(kx - \sigma t) + \alpha_2], \quad \text{(B5)}$$

where $|\eta_2| = A_1\{B^2{}_1 + B^2{}_2\}^{1/2}$, and $\alpha_2 = \tan^{-1}(B_2/B_1)$, with the principal value to be taken if $B_1 > 0$, and π plus the principal value if $B_1 < 0$.

Figures

Click on thumbnail for full-sized image.

Fig. 1. The geometry of the analytical model. The upper boundary at $z = h$ is a rigid surface. The incident wave has wavenumber $(k, -m)$ and travels in a direction with group velocity vector at angle β to the horizontal so that $\tan\beta = k/m$. It produces a disturbance $z = \eta(x, t)$ at the interface across which there is a density discontinuity, $\Delta\rho$, between the lower layer, where N is constant, and the upper layer, where the density is uniform.

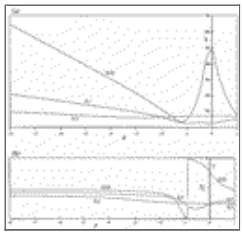

Click on thumbnail for full-sized image.

Fig. 2. (a) The interfacial wave nonlinear parameter χ and (b) the angle $\gamma = \alpha_1 - \alpha_2$, which defines the wave shape (see text), for varying p at $t_\beta = \tan\beta = 0.1$ and values of $t_{kh} = \tanh kh = 0.03$, 0.1, and 0.3, as marked on the curves.

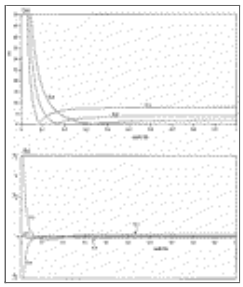

Click on thumbnail for full-sized image.

Fig. 3. (a) The interfacial wave nonlinear parameter χ and (b) the angle $\gamma = \alpha_1 - \alpha_2$, which defines the wave shape (see text), for varying $t_{kh} = \tanh kh$ at $p = 0.2$ ($\sigma_0/\sigma = 0.89$) and values of $t_\beta = \tan\beta = 0.1$, 0.2, and 0.4 ($\beta = 5.7°$, 11.3°, and 21.8°, respectively) as marked on the curves.

Corresponding author address: Dr. S. A. Thorpe, Department of Oceanography, University of Southampton, Southampton Oceanography Centre, European Way, Southampton SO14 3ZH, United Kingdom.

top

© 2008 American Meteorological Society Privacy Policy and Disclaimer
Headquarters: 45 Beacon Street Boston, MA 02108-3693
DC Office: 1120 G Street, NW, Suite 800 Washington DC, 20005-3826
amsinfo@ametsoc.org Phone: 617-227-2425 Fax: 617-742-8718
Allen Press, Inc. assists in the online publication of *AMS* journals.